Model-Based Analysis of the Ballistocardiogram Signal During Obstructive and Central Apnea

Arthur Ben-Tolila[1], Virginie Le Rolle[1], Alfredo I Hernández[1]

[1] Univ Rennes, Inserm, LTSI - UMR 1099, F-35000 Rennes, France

Abstract

The ballistocardiogram (BCG) is the signal generated by body micromovements resulting from the ejection of blood from the heart. Recent research highlights its potential for unobtrusive monitoring of sleep-disordered breathing. Although obstructive and central apneas affect the BCG signal, the mechanisms behind these variations are still under debate. An integrated model of cardio-respiratory interactions was adapted to study BCG behavior around both apnea types. The Morris sensitivity analysis was applied to identify most relevant parameters. Influent model parameters were related to ventricular and arterial function, as well as CO_2 sensitivity. These findings illustrate the cardiorespiratory information contained in this signal, and these parameters can be used in future work for patient-specific modeling.

1. Introduction

Sleep apnea syndrome (SAS) is characterised by repeated respiratory pauses and reductions during sleep. The resulting intermittent hypoxia and sleep fragmentation has long-term deleterious consequences on the cardiovascular system, including hypertension and heart disease. In obstructive SAS (OSAS), apneas are caused by upper airway collapse with continued breathing effort [1], while central SAS (CSAS) occurs due to decreased respiratory drive. The appropriate detection and differentiation of central and obstructive events during polysomnography (PSG) is necessary to orient the clinician towards the appropriate therapeutic options for each patient [2].

The ballistocardiogram (BCG) signal represents the body micromovements resulting from the ejection of blood from the heart. It is modulated by respiration, and its measurement is fully non-invasive; interest is growing for its use in SAS monitoring. The effects of obstructive and central apneas appear distinguishable [3], as the respiratory variations of BCG are correlated to intrathoracic pressure [4]. However, to our knowledge, few works have investigated the mechanisms behind these differences.

Models of the BCG signal have recently been proposed to study the influence of cardiac and circulatory parameters on its modulations [5–7]. However, they do not simulate the respiratory or nervous systems: they are not suited to the study of SAS, which relies on interactions between the cardiac and respiratory regulatory systems. This work therefore aims: 1) to adapt an integrated cardio-respiratory model, developed by our team and validated for the simulation of SAS in adults [8, 9], to synthesise a BCG signal, and 2) to investigate the influence of cardiac and respiratory parameters on BCG dynamics around simulated central and obstructive apneas, using a sensitivity analysis.

2. Methods

2.1. Model description

The closed-loop integrated model of cardio-respiratory interactions used in this work was developed by Guerrero et al. [8, 9]. It includes *i)* the cardiovascular and *ii)* respiratory systems, *iii)* gas exchanges, and *iv)* neural control.

i) Cardiovascular system. This model includes a pulsatile heart with the four cavities, as well as the systemic and pulmonary circulations (fig. 1). The *cardiac electrical activity* is modeled using cellular automaton, activating the contraction of their respective chamber [10] through elastance driving functions, one for the atria, and one for the ventricles $e_V(t)$ ($V \in \{LV, RV\}$):

$$e_V(t) = C \cdot \left(\frac{\left(\frac{t}{\alpha_1 T}\right)^{n_1}}{1 + \left(\frac{t}{\alpha_1 T}\right)^{n_1}} \right) \cdot \left(\frac{1}{1 + \left(\frac{t}{\alpha_2 T}\right)^{n_2}} \right) \quad (1)$$

where C is a positive constant, T is the heart period, and n_1, n_2, α_1 and α_2 are model parameters [11]. Ventricular blood pressure P_V is calculated using the end-systolic P_{es} and end-diastolic P_{ed} pressures:

$$P_v(V_V, t) = e_V(t) \cdot P_{es}(V_V) + (1 - e_V(t)) \cdot P_{ed}(V_V) + P_{thor} \quad (2)$$

$$P_{es}(V_V) = E_{v,es} \cdot (V_V - V_{u,V}) \quad (3)$$

$$P_{ed}(V_V) = P_0 \cdot (e^{\lambda \cdot (V_V - V_0)} - 1) \quad (4)$$

 ISSN: 2325-887X DOI: 10.22489/CinC.2024.234

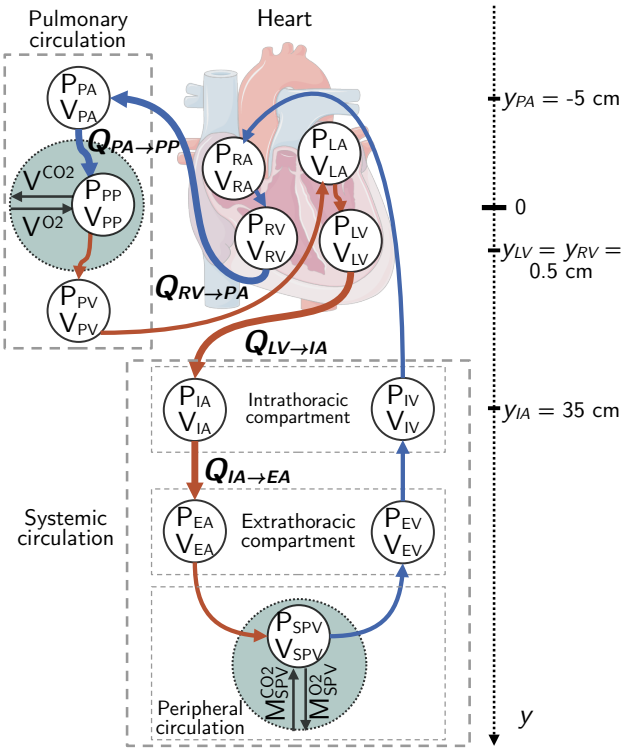

Figure 1: Cardio-vascular submodel. Blood flows Q used to compute f_{BCG} (eq. 5) are indicated, as well as the coordinates y_i of the corresponding compartments in the heart-to-foot plane.

where $E_{V,es}$ is the end-systolic ventricular elastance, V_V the instantaneous ventricular volume, $V_{u,V}$ the unstressed ventricular volume, P_{thor} the thoracic pressure, and other symbols are model parameters. Finally, each *systemic and pulmonary circulatory compartment* is characterised by an unstressed volume V_u, elastance E, blood pressure P and blood volume V, with $P = E(V - V_u)$. They are connected with resistances R, ideal diodes modeling the heart valves around atrial and ventricular compartments, and an inductance L between the intra- and extrathoracic arteries. Blood flows between compartments are denoted Q.

ii) Respiratory system. It comprises the upper, intermediate and lower airways, the respiratory muscles, the pleural cavity, the chest wall and the alveolar compartment [9, 12]. Apneas are simulated at end-expiration, *central apneas* by setting the respiratory muscle activity to 0, and *obstructive apneas* by greatly increasing the upper airway resistance.

iii) Gas exchanges and transport. The systemic peripheral vessels compartment performs the *metabolic gas exchanges* using constant rates, as in [13]. The *lung gas exchange* submodel computes the arterial gas concentrations from the gas fractions in inspired air. O_2 and CO_2 concentrations are transmitted by the circulation using conservation of mass and delays. The conversion between gas concentrations and partial pressures are computed using the gas dissociation functions defined in [14].

iv) Neural control. The modeled *chemoreflex* [13] regulates the breathing rhythm and the respiratory muscle activity. It is separated into the peripheral chemoreflex, sensitive to changes in arterial gas partial pressures Pa_{O_2} and Pa_{CO_2}, and the central chemoreflex, sensitive to Pa_{CO_2}. The modeled *baroreflex* regulates the ventricular elastances, systemic resistances and unstressed venous volumes with sympathetic afferences, and the heart rate through sympathetic s and vagal v pathways. The latter is affected by lung volume through the pulmonary stretch receptors. Each baroreflex branch receives as input P_{IA} (fig. 1) after first-order filtering, and comprises a sigmoid normalisation function, a delay, and a first-order filter.

v) BCG signal modeling. The synthetic BCG signal was adapted from Guidoboni et al. [6] and built in a post-simulation stage. Considering the blood flows out of the left ventricle into the intrathoracic arteries $Q_{LV\rightarrow IA}$, from the intra- to the extrathoracic arteries $Q_{IA\rightarrow EA}$, from the right ventricle to the pulmonary artery $Q_{RV\rightarrow PA}$, and from the pulmonary artery into the pulmonary capillaries $Q_{PA\rightarrow PP}$, the BCG waveform f_{BCG} [g cm s^{-2}] was obtained by:

$$f_{BCG} = \rho_b \cdot \left(y_{LV} \frac{dQ_{LV\rightarrow IA}}{dt} + y_{IA} \frac{dQ_{IA\rightarrow EA}}{dt} + y_{RV} \frac{dQ_{RV\rightarrow PA}}{dt} + y_{PA} \frac{dQ_{PA\rightarrow PP}}{dt} \right) \quad (5)$$

where $y_c, c \in [LV, IA, RV, PA]$ denotes the coordinate of the respective compartment in the heart-to-foot axis (fig. 1), and ρ_b the blood density. To quantify the respiratory modulation of the BCG, the envelope of f_{BCG} was calculated as the amplitude of the J wave minus that of the I wave (fig. 2) for each heart beat, yielding the time series (E_{BCG}) which was resampled at 1024 Hz as $E_{BCG}(t)$ to match the sampling frequency of the simulation (fig. 3).

2.2. Sensitivity analysis

The sensitivity analysis of the 175 model parameters was performed using Morris's screening method [15], using 400 iterations, a grid of $p = 26$ levels, and exploring a parameter range of $\pm 20\%$ of their nominal value. The same random grid was used for the analysis of central and obstructive apneas. The importance of parameters i was ranked using the distance $D_i = \sqrt{(\mu_i^*)^2 + (\sigma_i)^2}$, where μ_i^* designates the mean of the absolute values of elementary effects, and σ_i their standard deviation. Output functions were defined as the mean and the standard deviation of the E_{BCG} signal, on three periods: 30 seconds before the apnea, during the 20-second apnea, and 30 seconds after the apnea.

3. Results and discussion

3.1. Baseline simulations

Fig. 2 shows the shape of the simulated BCG obtained during one cardiac cycle, with the main systolic (I, J, K) and diastolic (L, M, N) waves visible. The I-J amplitude is highlighted to indicate the value of the E_{BCG} sample for this cardiac cycle.

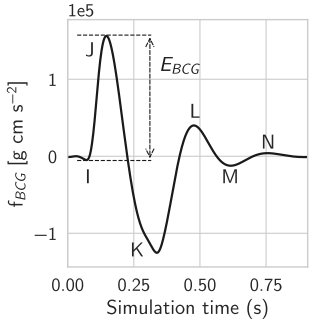

Figure 2: Simulated BCG waveform over one cardiac cycle, with its corresponding E_{BCG}.

The resampled E_{BCG} signal is shown in fig. 3, from 30 seconds before to 30 seconds after the apnea. Its respiratory modulation is visible, and its dynamics during apnea are consistent with the literature: the baseline and standard deviation increase during the increased respiratory effort generated by the obstructive apnea, and the respiratory oscillations are abolished during central apnea [4].

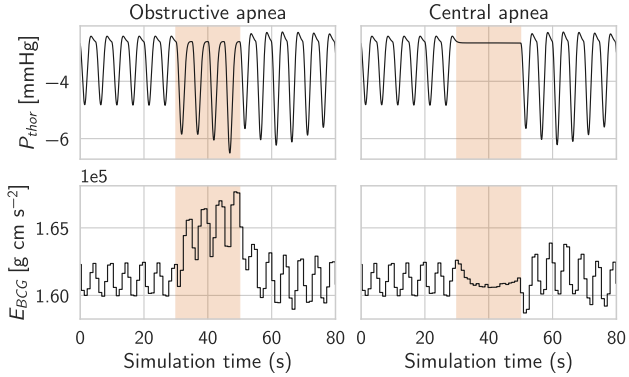

Figure 3: Thoracic pressure (P_{thor}, top line) and E_{BCG} (bottom line) during obstructive and central apnea, indicated by the solid red zone.

3.2. Sensitivity analysis results

Figures 4, 5 and 6 display the results for the sensitivity analysis of the mean and standard deviation of E_{BCG} during the apnea, respectively. Only the 9 most influent parameters are displayed for readability. As expected, the standard deviation of E_{BCG} is much smaller during the central apnea than during the obstructive apnea, and no influent parameters can be obtained. The influence of the time period (before, during and after the apnea) on the parameter classification for the mean E_{BCG} is very small, and is therefore not displayed. Results are also very similar for the standard deviation before and after the apnea.

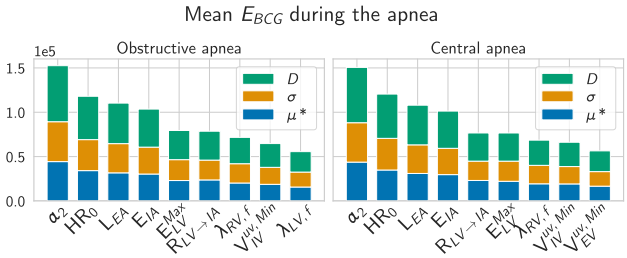

Figure 4: Results of the Morris sensitivity analysis for the mean E_{BCG} during obstructive (left) and central (right) apnea.

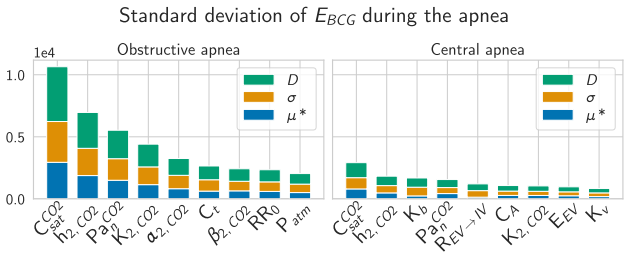

Figure 5: Results of the Morris sensitivity analysis for the standard deviation of E_{BCG} during obstructive (left) and central (right) apnea.

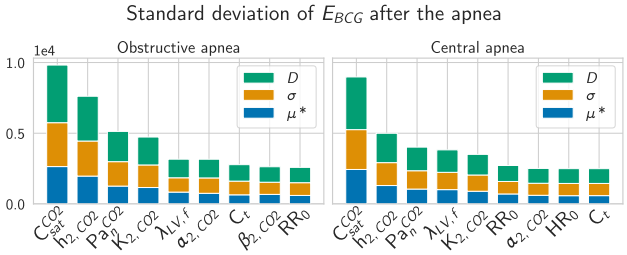

Figure 6: Results of the Morris sensitivity analysis for the standard deviation of E_{BCG} during obstructive (left) and central (right) apnea.

It is broadly accepted in the literature that the BCG I-J height is positively correlated to cardiac output (CO) [16]. Several groups of parameters appear influent on the mean E_{BCG} because they affect the CO with different mechanisms.

Ventricular elastance parameters α_2 (equation 1) and E_{LV}^{Max} (affecting $E_{LV,es}$, equation 3) regulate the maximal ventricular elastance, and therefore the cardiac contractility. If it decreases, the ejection force of the ventricles is lessened and results in a decreased BCG amplitude. Similar effects can be seen through the Frank-Starling mechanism by increasing the **baseline heart rate** HR_0. These observations are consistent with Inan et al.'s findings on BCG behavior during the Valsalva maneuver [17]. Parameters $\lambda_{LV,f}$ and $\lambda_{RV,f}$ affecting the end-diastolic ventric-

ular pressure P_{ed} (equation 4) also influence the CO, as an increased P_{ed} results in a decreased ventricular outflow.

Parameters of the **intra- and extrathoracic arteries** (indices IA and EA, respectively) affect the damping of the pressure and flow waves in these compartments. Stiffer (higher E_{IA}), less resistive arteries (lower R_{IA}) with less blood inertia (lower L_{EA}) transmit pressure waves with less damping between compartments, resulting in higher pressure gradients between compartments, therefore higher outflows and increased mean E_{BCG}. They are also less sensitive to respiratory modulation, showing a reduced standard deviation of E_{BCG}. These results are coherent with the literature, as Kim et al. [5] demonstrated with their BCG model that the pressure gradients in the aorta are the major contributors to the BCG waveform. Similarly, increasing the intra- and extrathoracic venous unstressed volumes $V_{IV}^{uv,min}$ and $V_{EV}^{uv,min}$ lowers the blood pressures downstream from the heart and arterial compartments, and therefore lowers the outflows and the BCG J wave height.

CO_2 sensitivity parameters are the major contributors to the standard deviation of E_{BCG}. Parameters C_{sat}^{CO2}, $K_{2,CO2}$, $h_{2,CO2}$, $\alpha_{2,CO2}$ and $\beta_{2,CO2}$ relate to the dissociation curve of the pulmonary CO_2, Pa_n^{CO2} is the set-point of the central chemoreceptors for the detection of arterial CO2 partial pressure, and C_t is involved in the afferent pathway to the peripheral chemoreceptors. These parameters influence the chemoreflex sensitivity to CO_2 changes. If it is increased, the amplitude of respiratory movements and the lung filling increases, and the respiratory modulation of E_{BCG} is more pronounced. During apnea, the desaturation becomes less profound, and the inspiratory effort during the obstructive apnea is increased. This results in a higher standard deviation of E_{BCG} around the apnea, and during the obstructive apnea. This corresponds to the findings of Polo et al. [4] of a linear correlation between BCG respiratory variation and intrathoracic pressure, as well as the flattening of this variation during central apnea.

4. Conclusion

An integrated cardio-respiratory model, previously validated for the study of SAS, was adapted to simulate a BCG signal. A group of parameters was identified as the most influent on BCG variations around obstructive and central apneas, paving the way towards patient-specific modeling and digital twin approaches in the context of SAS.

References

[1] Lévy P, et al. Obstructive sleep apnoea syndrome. Nature Reviews Disease Primers 2015;1(1):15015.

[2] Baillieul S, et al. Diagnosis and management of central sleep apnea syndrome. Expert Review of Respiratory Medicine 2019;13(6):545–557.

[3] Balali P, et al. Investigating cardiorespiratory interaction using ballistocardiography and seismocardiography — a narrative review. Sensors 2022;22(23):9565.

[4] Polo O, et al. Respiratory variation of the ballistocardiogram during increased respiratory load and voluntary central apnoea. Eur Respir J 1992;5(2):257–262.

[5] Kim CS, et al. Ballistocardiogram: Mechanism and potential for unobtrusive cardiovascular health monitoring. Sci Rep 2016;6(1):31297.

[6] Guidoboni G, et al. Cardiovascular function and ballistocardiogram: A relationship interpreted via mathematical modeling. IEEE Trans Biomed Eng 2019;66(10):2906–2917.

[7] Rabineau J, et al. Closed-loop multiscale computational model of human blood circulation. Applications to ballistocardiography. Frontiers in Physiology 2021;12.

[8] Guerrero G, et al. Parametric Analysis of an Integrated Model of Cardio-respiratory Interactions in Adults in the Context of Obstructive Sleep Apnea. Ann Biomed Eng 2021;49(12):3374–3387.

[9] Guerrero G, et al. Modeling patient-specific desaturation patterns in sleep apnea. IEEE Trans Biomed Eng 2022; 69(4):1502–1511.

[10] Hernández AI, et al. Model-based interpretation of cardiac beats by evolutionary algorithms: signal and model interaction. Artif Intell Med 2002;26(3):211–235.

[11] Guerrero G. Analyse à base de modèles des interactions cardiorespiratoires chez l'adulte et chez le nouveau-né. Ph.D. thesis, Université de Rennes 1, LTSI - INSERM U1099, 2020.

[12] Le Rolle V, et al. Mathematical modeling of respiratory system mechanics in the newborn lamb. Acta Biotheor 2013; 61(1):91–107.

[13] Albanese A, et al. An integrated mathematical model of the human cardiopulmonary system: model development. Am J Physiol Heart Circ Physiol 2016;310(7):H899–H921.

[14] Spencer JL, et al. Computational expressions for blood oxygen and carbon dioxide concentrations. Annals of Biomedical Engineering 1979;7(1):59–66.

[15] Morris M. Factorial sampling plans for preliminary computational experiments. Technometrics 1991;33(2):161–174.

[16] Giovangrandi L, et al. Ballistocardiography – a method worth revisiting. In Conference proceedings of the Annual International Conference of the IEEE Engineering in Medicine and Biology Society, volume 2011. 2011; 4279–4282.

[17] Inan OT, et al. Robust ballistocardiogram acquisition for home monitoring. Physiological Measurement 2009; 30(2):169–185.

Address for correspondence:

Virginie Le Rolle
Université de Rennes, LTSI, Rennes, 35042, France
virginie.lerolle@univ-rennes.fr